STATIC AND TRANSIENT BEAM LOADING OF A SYNCHROTRON

BOOSTER TECHNICAL NOTE
NO. 208

S. Y. Zhang and W. T. Weng

July 8, 1992

ALTERNATING GRADIENT SYNCHROTRON DEPARTMENT
BROOKHAVEN NATIONAL LABORATORY
UPTON, NEW YORK 11973

STATIC AND TRANSIENT BEAM LOADING OF A SYNCHROTRON *

S.Y. Zhang and W.T. Weng

AGS Department, Brookhaven National Laboratory,
Upton, New York 11973

ABSTRACT

In a synchrotron, when the beam induced current is comparable to the driver current, the RF cavity is subjected to beam loading perturbation and corrective steps have to be implemented to regain beam stability.

In this paper, the static and transient beam loading will be studied. We first discuss the static beam loading, which includes the cavity detuning condition, the stability condition, and the generator power dissipation. The beam current induced beam phase deviation is used as criterion to study the transient beam loading. The upgraded and the old AGS RF system parameters are used as an example to demonstrate how to choose cavity and generator parameters to satisfy the stability requirements under the beam loading.

The dynamic models for the beam loading with beam control, and the beam loading with fast power amplifier feedback are presented and analyzed. It is shown that the beam phase and radial feedbacks alone are insufficient for the transient beam loading compensation, but the fast power amplifier feedback can provide effective correction on the beam loading. The limitation of the fast feedback and the beam loading with tuning and AVC loops are also discussed.

* Work performed under the auspices of the U.S. Department of Energy

I. Introduction

When a high intensity beam passes through an RF cavity, the beam-induced image wall current will affect the cavity voltage, then the beam itself will be affected by the variation of the cavity voltage. Such effects are called the beam loading in accelerator technology.

In this report, two beam loading effects will be studied, one is the static beam loading and another is the transient beam loading. The static beam loading applies when all RF buckets are filled with beam and a steady state condition has been established, and the transient beam loading applies when the bunch train first passes through the cavity and before a steady state condition is established.

The most important components in the beam loading are the RF cavity and the generator, which together determine the loaded cavity impedance. Using the results from the study of the static and transient beam loading, the parameters of the cavity and generator can be evaluated. Once a cavity and a generator have been chosen, the tuning and AVC loops are needed to guarantee the working condition for the generator and the cavity. Other techniques such as the fast power amplifier feedback, the feedforward compensation, and the beam phase and radial feedbacks can be properly used to alleviate the beam loading effects.

In this paper, we discuss the beam loading at one of the worst case, i.e., the bunched beam box-car injection from one synchrotron to another.

II. Cavity and Generator

Schematically the loaded cavity can be represented by a lumped RLC circuit as shown in Fig.1, where the generator impedance is included in the shunt resistance R. Therefore, the parameters of the loaded cavity are determined by both the RF cavity and the generator. The RF driver current and the beam loading current are represented by current sources I_G and I_B, respectively. Note that I_B is the fundamental component of the beam-induced image current. Here the fundamental frequency implies the RF frequency.

Taking the current as the input and the resulting cavity voltage V as the output, the transfer function of the cavity $Z(s)$ is shown as,

$$V = Z(s)\, I = \frac{\frac{s}{C}}{s^2 + \frac{1}{RC}s + \frac{1}{LC}}\, I \tag{1}$$

Using the resonant frequency,

$$\omega_R = \frac{1}{(LC)^{1/2}} \tag{2}$$

and the cavity half bandwidth,

$$\sigma = \frac{1}{2RC} \tag{3}$$

the transfer function $Z(s)$ in (1) can also be written as,

$$Z(s) = \frac{2\sigma R s}{s^2 + 2\sigma s + \omega_R^2} \tag{4}$$

If the cavity is driven by a sine wave whose frequency coincides with the resonant frequency, i.e., $s = j\omega_R$, the impedance of the cavity is simply $Z = R$. The current $I = V/R$ is provided by the generator, and the power dissipated in the cavity is,

$$P = \frac{1}{2\pi}\int_0^{2\pi} \frac{(V\sin\alpha)^2}{R} d\alpha = \frac{V^2}{2R} \tag{5}$$

The energy stored in the cavity can be represented by,

$$W = \frac{CV^2}{2} \tag{6}$$

The equations (5) and (6) indicate that for a certain voltage V the shunt resistance R determines the power dissipation, and the capacitance C determines the energy stored in the cavity. These two parametors are important in the static and transient beam loading.

In the vector form, the cavity impedance can be written as,

$$Z = R\cos\phi\ e^{-j\phi} \tag{7}$$

where

$$\phi = \tan^{-1}\left(Q\left(\frac{\omega_R}{\omega} - \frac{\omega}{\omega_R}\right)\right) \tag{8}$$

is the detuning angle and Q is the quality factor of the loaded cavity,

$$Q = R(\frac{C}{L})^{1/2} \tag{9}$$

If $\Delta\omega = \omega_R - \omega << \omega_R$, then (8) can be simplified as,

$$\phi = \tan^{-1}(2Q\frac{\Delta\omega}{\omega_R}) \tag{10}$$

Substituting (10) into (7), we get,

$$Z = \frac{R}{1 + j2Q\,\Delta\omega/\omega_R} \tag{11}$$

III. Static Beam Loading

In the static beam loading, the cavity has to be detuned and the power amplifier has to be set at an adequate condition to accommodate the passing beam. The subjects of interest include the detuning condition, the stability condition, and the power dissipation of the generator.

1. Detuning Condition

In the absence of beam, the cavity is driven by I_{G0}, and the cavity voltage is simply $V = I_{G0}R$. This is shown in Fig.2, where the beam current $\bar{I}_B$ and the stable phase ϕ_S are also shown. Note that we consider the beam loading below transition.

With the beam loading, one way to keep the cavity voltage unchanged is to detune the cavity by an angle, say ϕ_Z, and to choose a proper generator current I_G [1], as shown in Fig.2. We assume that I_G is still in the same phase as V, which can be accomplished by a cavity detuning, or automatically by the tuning loop. Meanwhile the amplitude of the cavity voltage V can be kept unchanged by the AVC loop. Using (7), this implies,

$$|I_T R\cos\phi_Z\ e^{-j\phi_Z}| = V = I_{G0}R \tag{12}$$

which is equivalent to,

$$I_T\cos\phi_Z = I_{G0} \tag{13}$$

where I_T is the total current. From Fig.2 we have,

$$I_B\ e^{-j(\frac{\pi}{2}+\phi_S)} + I_G = I_T\ e^{-j\phi_Z} \tag{14}$$

Combining (13) and (14), and equating the real and imaginary parts separately, we have the following condition specifying the detuning angle ϕ_Z and the generator current I_G for the cavity detuning,

$$\tan\phi_Z = Y\cos\phi_S \tag{15}$$

$$I_G = I_{G0} + I_B\sin\phi_S \tag{16}$$

where the ratio of the beam current to the original generator current,

$$Y = \frac{I_B}{I_{G0}} \tag{17}$$

is important in determining the stability condition, which will be shown in the following subsection.

2. Stability Condition

The stability problem has been resolved for the case of beam loading without feedback loops by Robinson [2]. A different way of arriving at the stability criteria, using Pedersen's model [3], will be presented here.

1. Robinson Stability Criteria

It is known, for example in [4], that the beam transfer function $T_1(s)$ from the cavity phase deviation $\Delta\phi_C$ to the beam phase deviation $\Delta\phi_B$ is shown in,

$$\Delta\phi_B = T_1(s)\Delta\phi_C = \frac{\Omega_S^2}{s^2+\Omega_S^2}\Delta\phi_C \tag{18}$$

where Ω_S is the synchrotron oscillation frequency.

The beam loading can be represented by the reaction of the cavity voltage to the beam current. If the cavity is detuned by a large amount, then this reaction has both phase and amplitude effects. In Pedersen's model, the phase deviation of the cavity voltage due to the beam phase deviation is as follows,

$$\Delta\phi_C = T_2(s)\Delta\phi_B = \frac{Y\sigma^2\tan\phi_Z/\cos\phi_S}{s^2 + 2\sigma s + \sigma^2(1+\tan^2\phi_Z)}\Delta\phi_B \tag{19}$$

Thus, the characteristic equation of the closed-loop dynamic system under beam loading is,

$$T_1(s)T_2(s) - 1 = 0 \tag{20}$$

which can be written as,

$$\begin{aligned} &s^4 + 2\sigma s^3 + (\sigma^2(1+\tan^2\phi_Z) + \Omega_S^2)s^2 + 2\sigma\Omega_S^2 s \\ &+ \sigma^2(1+\tan^2\phi_Z)\Omega_S^2 - Y\Omega_S^2\sigma^2\tan\phi_Z/\cos\phi_S = 0 \end{aligned} \tag{21}$$

The Routh-Hurwitz table [5] corresponding to equation (21) is produced as follows,

s^4	1	$\sigma^2(1+\tan^2\phi_Z)+\Omega_S^2$	$\sigma^2\Omega_S^2(1+\tan^2\phi_Z - Y\frac{\tan\phi_Z}{\cos\phi_S})$
s^3	2σ	$2\sigma\Omega_S^2$	
s^2	$\sigma^2(1+\tan^2\phi_Z)$	$\sigma^2\Omega_S^2(1+\tan^2\phi_Z - Y\frac{\tan\phi_Z}{\cos\phi_S})$	
s^1	$\frac{2\sigma\Omega_S^2 Y\tan\phi_Z}{(1+\tan^2\phi_Z)\cos\phi_S}$		
s^0	$\sigma^2\Omega_S^2(1+\tan^2\phi_Z - Y\frac{\tan\phi_Z}{\cos\phi_S})$		

To guarantee the stability, all entries in the first coefficient column should be positive. The fourth entry therefore requires,

$$\tan\phi_Z > 0 \tag{22}$$

and the fifth entry requires,

$$Y\tan\phi_Z\cos^2\phi_Z < \cos\phi_S \tag{23}$$

The conditions (22) and (23) are called the first and second Robinson stability criteria, respectively. In the following we will discuss the physical meanings of the criteria.

2. Robinson Resistance

Recalling the cavity detuning condition (15), since $0 \leq \phi_S < \pi/2$, and hence $\cos\phi_S > 0$, the first Robinson condition ia always satisfied if a tuning loop is applied. Substituting the detuning condition (15) into the second criterion (23), we get,

$$Y\sin\phi_S < 1 \tag{24}$$

Substituting $Y = I_B/I_{G0}$ and $I_{G0} = V/R$ into (24) and defining the Robinson resistance,

$$R_R = \frac{V}{I_B \sin\phi_S} \tag{25}$$

the second Robinson criterion becomes,

$$R < R_R \tag{26}$$

Since the shunt resistance R includes the generator impedance, therefore for a given R_R, reducing the generator impedance is always an effective means to increase the stability margin.

Finally, we note that the equation (26) represents the second Robinson criterion under the condition that the detuning condition (15) is satisfied. Under other detuning conditions, it cannot be used.

3. More On the Second Robinson Criterion

On the stability limit of the second Robinson criterion, from (17) and (24) we can write,

$$I_{G0} = I_B \sin\phi_S \tag{27}$$

Under the condition (27), Fig.2 can be redrawn as Fig.3. It is shown clearly that in this case $I_T = I_B$ and $\phi_Z = \pi/2 - \phi_S$. The generator voltage V_G is in the opposite direction with the beam image current I_B, and it is therefore collinear with the beam current $\bar{I}_B$. In other words, the bunch now sits on the crest of the generator voltage. Since the generator voltage is the only recovery force, this explains why the condition (27) is a stability limit. Meanwhile, from Fig.3 we may find that,

$$I_G = 2I_{G0} \tag{28}$$

Substituting (28) into (16), we also obtain (27).

3. Power Dissipation

The power dissipation of the generator often poses a severe limitation on the operation

of the RF system. This problem is considered in this section for the general situation, where the cavity is not necessarily detuned according to the condition (15). To keep the phase and amplitude of the total cavity voltage V unchanged, the generator current I_G can be in a different phase ϕ_L with the cavity voltage, as shown in Fig.4. In other words, the problem now is that given an arbitrary detuning angle ϕ_Z, to find proper I_G and ϕ_L such that,

$$I_T \cos\phi_Z = I_{G0} \tag{29}$$

Note that from Fig.4, we have,

$$I_B \; e^{-j(\frac{\pi}{2} + \phi_S)} + I_G \; e^{j\phi_L} = I_T \; e^{-j\phi_Z} \tag{30}$$

By equating separately the real and imaginary parts in (30), we get the following equations,

$$\tan\phi_Z = Y\cos\phi_S - \tan\phi_L - Y\sin\phi_S\tan\phi_L \tag{31}$$

$$I_G = (I_{G0} + I_B\sin\phi_S)/\cos\phi_L \tag{32}$$

There are two extreme situations. If the cavity is detuned according to (15), then we have $\phi_L = 0$, and if the cavity is not detuned at all, then we have $\phi_Z = 0$. From (32), it is clear that the generator current reaches the minimum if the cavity is detuned according to (15), i.e., $\phi_L = 0$. This is the reason why a tuning loop is necessary in the operation for most RF systems.

The total power delivered by the generator can be calculated as,

$$P_T = \frac{1}{2} I_G V_G = \frac{1}{2} I_G^2 R \cos\phi_Z \tag{33}$$

If the cavity is fully detuned, substituting (15) and (16) into (33), we get,

$$P_T = (\frac{V^2}{2R} + I_B V\sin\phi_S + \frac{RI_B^2 \sin^2\phi_S}{2}) \, (1 + (\frac{I_B R}{V})^2 \cos^2\phi_S)^{-1/2} \tag{34}$$

Under the condition of $I_{G0} >> I_B$, or $V >> I_B R$, the total power delivered by the generator can be written as,

$$P_T = \frac{V^2}{2R} + I_B V\sin\phi_S \tag{35}$$

where the first term is the power dissipated in the cavity, and the second term represents the power delivered to the beam.

IV. Transient Beam Loading

There are two methods in studying the transient beam loading. The first one is to look at the cavity voltage variation due to the beam loading. The second one, we consider that the most sensitive effect of the beam loading can be represented by the beam current-induced beam phase deviation, therefore the transfer from the beam current to the induced beam phase deviation can be used. Here we adopt the second method.

We assume that the beam enters the cavity without phase error, as shown in Fig.5a, where the beam phase equals the stable phase ϕ_S, and therefore the beam phase deviation with respect to the phase of the cavity voltage $\Delta\phi = 0$. As soon as the beam induced cavity voltage component V_B builds up, the total cavity voltage V no longer equals V_G, and the beam phase deviation changes from zero to $\Delta\phi = -\phi_Z$, as shown in Fig.5b. Note that this deviation is generated from the variation of the cavity voltage, not from the beam motion. Also note that since the tuning loop and the AVC loop are relatively slow, we assume that the cavity is not detuned and also the generator current is not changed, during the short period of beam injection.

It is shown in Fig.5b that the cavity voltage component V_B is directly responsible to ϕ_Z, and hence the beam phase deviation $\Delta\phi$. The response of V_B to the beam image current I_B, however, is governed by the cavity transfer function $Z(s)$ in (1). If we consider the transfer function from I_B to ϕ_Z, then the dynamic aspect of the transfer can be represented by,

$$Z_1(s) = \frac{\sigma}{s + \sigma} \tag{36}$$

where σ is the cavity half bandwidth, as defined by equation (3). In Fig.6, the response by using $Z_1(s)$ for a step input is shown, comparing to the cavity voltage response due to an

exciting sine current with the resonant frequency using $Z(s)$. Two responses share the same time constant.

For the scaling, we consider under the assumption that ϕ_S is small,

$$\tan\phi_Z \approx \frac{I_B}{I_{G0}} \tag{37}$$

If furthermore $\frac{I_B}{I_{G0}} \leq 1$, then we get,

$$\phi_Z \approx Z_0 I_B = \frac{1}{I_{G0}} I_B \tag{38}$$

If $\frac{I_B}{I_{G0}} > 1$, then Z_0 has to be numerically calculated.

To use the cavity model $Z_1(s)$, for a continuous beam injection, I_B can be a step function, as shown in Fig.6. After the ring filled, the circulating beam replaces the injected beam. The real beam current is the sum of the originally injected beam and the variant portion of the following beam. In this study, we use I_{B0} to denote the invariant portion of the beam, which can also be seen as the initial beam loading condition.

The total response from I_{B0} to the beam phase deviation can therefore be shown as,

$$\Delta\phi = -\phi_Z = Z_1(s) Z_0 I_{B0} \tag{39}$$

The equation (39) shows that both $Z_1(s)$ and Z_0 are relevant to the beam loading impact on the beam phase deviation. Since $Z_0 = 1/I_{G0}$ and $I_{G0} = V/R$, reducing R can reduce the beam loading effect. This is consistent with the results of the static beam loading, where it has been shown that by reducing R, and therefore increasing the power dissipation P, the stability margin can be increased. For $Z_1(s)$, if the cavity half bandwidth σ is increased, the response of the beam phase deviation to the beam loading will be more sensitive, which will happen if R is reduced. To solve the problem, the capacitance C can be increased to keep σ not increased. Recalling (6), this implies to increase the cavity stored energy W.

V. AGS Beam Loading Parameters

Using the results of the static and transient beam loading study, the cavity and generator parameters can be chosen to satisfy the stability requirements for the beam loading.

In the new operation, the proton beam intensity at the AGS will be increased from 1.5×10^{13} to 6×10^{13} per cycle. Also, the AGS ring will directly receive the bunched beam from the Booster. Therefore, the old cavities and power amplifiers have to be upgraded. In the following, we show the beam loading parameters for the old and the upgraded AGS RF systems. Some information are taken from [6] and [7].

AGS BEAM LOADING PARAMETERS						
Notation	AGS-OLD		AGS-NEW		Unit	Formulae
	Inj.	Ext.	Inj.	Ext.		
f	4.2	4.5	4.2	4.5	MHz	
V	32	32	40	40	KV	
Q	21	20	19	19	1	
C	82	82	175	175	pF	
L	17.5	15.3	8.2	7.15	μH	$\omega_R=(LC)^{-1/2}$
R	9.7	8.6	4.2	3.8	$K\Omega$	$R=Q/(\omega_R C)$
I_{G0}	3.3	3.7	9.52	10.52	A	$I_{G0}=V/R$
I_B	7.91	8.5	7.91	8.5	A	$I_B=nqf \times \pi/2$
Y	2.4	2.3	0.83	0.81	1	$Y=I_B/I_{G0}$
ϕ_S	0	30	0	30	degree	
I_G	3.3	7.95	9.52	14.78	A	$I_G=I_{G0}+I_B\sin\phi_S$
ϕ_Z	67.4	-63.3	39.7	-35	degree	$\tan\phi_Z=I_B/I_{G0} \times \cos\phi_S$
Δf	240.2	-223.7	91.8	-82.9	KHz	$\Delta f=f\tan\phi_Z/(2Q)$
R_R	∞	7.5	∞	9.4	$K\Omega$	$R_R=V/(I_B\sin\phi_S)$

The AGS RF harmonic number is 12, and there are 10 RF cavities in the AGS ring. The presented parameters are for each cavity. The number of protons in one bunch, n, is assumed to be 0.75×10^{13}, a 50 percent larger than the designed number.

The resonant frequency ω_R and the quality factor Q for the loaded cavity can be accurately measured. The measurement of the cavity capacitance is usually not accurate, but the data can be used with an adjustment according to experience. The rest of the parameters can then be calculated according to the formulae shown in the table.

In the upgrade, the two most important modifications are reducing the loaded cavity shunt resistance R, and increasing the capacitance C. By reducing R, the generator current I_{G0} is increased. The ratio of the beam current and the generator current Y is significantly reduced, which then requires a smaller detuning angle. The price paid is that more powerful power amplifiers are required. By increasing the cavity capacitance C, the cavity bandwidth is kept almost unchanged in the upgrade.

At the injection, i.e., $f = 4.2\ MHz$, the Robinson resistance is infinity. Attention should be paid in this case when the criterion (26) is used, because the desired detuning according to (15) may not be guaranteed.

VI. Beam Loading with Beam Control

Several techniques may be applied to reduce the beam loading effect, such as the phase and radial feedbacks, the fast power amplifier feedback, and the feedforward compensation. In the following sections, we show the advantages and limitations of these techniques.

First, we consider the beam loading with beam control. The model is shown in Fig.7. The loop encircling b/s, a, and $1/s$ represents the beam synchrotron oscillation, with,

$$a = -\frac{\omega_{id}\eta\gamma_T^2}{R_0} \tag{40}$$

where ω_{id} is the ideal beam frequency, η is the frequency slip factor, γ_T is the beam transition energy, and R_0 is the mean radius of the accelerator, and also with,

$$b = -\frac{eV\cos\phi_S c}{2\pi\gamma_T^2\beta E} \tag{41}$$

where β is the ratio of the particle velocity v and the light velocity c, and E is the total energy of the proton.

The synchrotron oscillation frequency therefore is,

$$\Omega_S = (-ab)^{1/2} = \left(-\frac{\omega_{id}\, eV\eta\cos\phi_S c}{2\pi r\beta E}\right)^{1/2} \tag{42}$$

ΔR and $\Delta\omega_B$ are the deviations of the beam radius and frequency from the synchronous condition, respectively. The total beam deviation $\Delta\phi$ is the difference between the beam phase deviation, $\Delta\phi_B$, and the cavity voltage phase deviation ϕ_Z, as shown in Fig.7. In this article, two types of beam phase deviations have been considered. One is the beam phase deviation with respect to that of cavity voltage, $\Delta\phi$, another one is the beam phase deviation with respect to ideal beam phase, $\Delta\phi_B$. The location and effect of these two errors can best be understood through Fig.7.

The loop encircling $Z_1(s)$, k_1, and $1/s$ represents the phase feedback. The total beam phase deviation $\Delta\phi$ is detected, and amplified to drive the VCO, which is represented here by the integrator $1/s$. The output of the VCO generates the generator current to drive the cavity. The response of the cavity voltage to the current, as discussed above, is represented by the transfer function $Z_1(s)$. This explains the phase feedback that includes the dynamic of the cavity. On the other hand, the beam loading current I_{B0} affects the cavity voltage by directly driving $Z_1(s)$, as shown in Fig.7.

Finally, the loop encircling b/s, k_2, k_1, $1/s$, and $Z_1(s)$ is the radial feedback loop. For the transient response, the contribution of this loop is not as significant as the phase loop because of an additional delay from b/s.

Note that the model for transient beam loading does not include the feedback of the beam phase deviation $\Delta\phi_B$ to the cavity voltage phase, as given in (19). This loop has been used for the study of the static stability. Since the response of this loop is slower than that of the phase and radial loops, the influence of this loop for the transient beam loading presented here can be disregarded.

Using (36) and (39), the beam phase deviation $\Delta\phi$ due to the beam loading I_{B0} is,

$$\Delta\phi = \frac{-\sigma Z_0 s^2}{s^3 + \sigma s^2 + (k_1\sigma + \Omega_S^2)s + \Omega_S^2\sigma + bk_1k_2\sigma} I_{B0} \tag{43}$$

We assume that all initial deviations of the beam are zero. When the bunched beam enters the cavity, the induced beam image current, scaled by Z_0, drives the cavity, which is

represented by $Z_1(s)$, to generates a cavity voltage phase variation $-\phi_Z$. Since we assume that the initial $\Delta\phi_B$ is zero, the beam phase deviation is momentarily equal to $-\phi_Z$. The phase feedback loop has a wider bandwidth than that of the synchrotron oscillation loop and the radial feedback loop, therefore, for the transient beam loading, we only consider the phase feedback.

An obvious means to reduce the beam loading impact is to increase the gain of the phase feedback, k_1. The typical phase loop bandwidth at the AGS is between 10 KHz to 100 KHz, corresponding to k_1 being between 63×10^3 to 63×10^4. At the injection, $a = 1.9 \times 10^6$, and $b = -74$, and therefore the synchrotron oscillation frequency is 1.89 KHz. For the new AGS RF cavity, the shunt resistance of the loaded cavity is 4.2 $K\Omega$ and the capacitance is 175 pF for each cavity, therefore we have $\sigma = 68 \times 10^4$ $rad/$sec. The cavity voltage amplitude is 40 KV. We choose a low phase feedback gain $k_1 = 4 \times 10^4$ and a radial feedback parameter $k_2 = 300$. The responses of the beam phase deviation for continuous injection with each bunch having 0.75×10^{13} protons are shown in Fig.8. It shows that in the period of 10 μs, the phase feedback provides a small phase correction. Such a phase feedback, however, will cause a significant emittance blow up as shown in the follows.

Taking the AGS parameters at the injection, i.e., $\beta = 0.925$, $E = 2.473$ GeV, $\eta = -0.13$, $\omega_{id} = 2\pi \times 4.14 \times 10^6$, and $h = 12$, the RF bucket half height equals,

$$H_{BK} = 2\,(\frac{eV\beta^2 E}{2\pi h\,\eta\omega_{id}^2})^{1/2} = 0.71\ eVs \tag{44}$$

It can be shown that RF bucket vertical motion in the frequency deviation reaches 4.4 KHz in about 6 μs. From the relation of the frequency deviation $\Delta\omega$ to the bucket half height,

$$H_{BK} = \frac{\beta^2 E}{\omega_{id}^2 \eta}\,\Delta\omega \tag{45}$$

the 4.4 KHz frequency deviation is equivalent to a bucket motion of 0.64 eVs, which is about 90 percent of the bucket half height and therefore implies an unacceptable beam emittance blow up. The bunch motion in the bucket is shown in Fig.9 by the solid line,

where the vertical axis represents the percentage of the bucket half height. To increase the gain of the phase feedback will further deteriorate the situation. Thus, we may conclude that for transient response, the compensation using the phase loop is limited and therefore not effective.

For a long period of time, however, a properly designed phase and radial feedback can correct the radial deviation and damp the phase deviation, and therefore they are still needed.

VII. Beam Loading with Fast Power Amplifier Feedback

The beam loading model with fast power amplifier feedback is shown in Fig.10. The feedback signal of the fast feedback is picked up at the cavity voltage, which in the model is equivalent to ϕ_Z, as discussed before. This signal is used to drive the power amplifier through a gain of k_0. Since this gain is included in the phase feedback path, therefore we divide the original phase feedback gain k_1 as $k_0\bar{k}_1$ as shown in Fig.10. It can be seen that the beam loading affects the cavity directly, while the fast feedback has to go through the power amplifier. Therefore from the beam loading point of view, the fast feedback gain k_0 is on the feedback path.

For the transient response of the beam loading, we may consider only the fast feedback and disregard other loops. With fast feedback, the transfer function corresponding to $Z_1(s)$ in (39) becomes,

$$Z_2(s) = \frac{\sigma}{s + (1 + k_0)\sigma} \tag{46}$$

The difference between $Z_2(s)$ and $Z_1(s)$ can be explained as follows. First, comparing the denominators of $Z_2(s)$ and $Z_1(s)$ and recalling $\sigma = 1/(2RC)$ in (3), we find that the effective shunt resistance of the cavity with fast feedback becomes $R/(1 + k_0)$. Therefore, the time constant of the cavity with the fast feedback is much smaller than that with $Z_1(s)$. Second, the static gain of the cavity with the feedback reduces by a factor of $1 + k_0$, which means

that the beam loading effect is significantly reduced by the fast feedback.

With fast power amplifier feedback, the beam loading effect due to I_{B0} becomes,

$$\Delta\phi = \frac{-\sigma Z_0 s^2}{s^3 + (1+k_0)\sigma s^2 + (k_1\sigma + \Omega_S^2)s + \Omega_S^2\sigma + bk_1k_2\sigma} I_{B0} \tag{47}$$

Taking a moderate fast feedback gain $k_0 = 5$, the response of the beam phase deviation under the same condition of that used in plotting Fig.8 is shown in Fig.11, where the residual phase error is reduced by a factor of 6. Also the bunch motion in the bucket is shown in Fig.9 by dotted line, which is much smaller than the motion with a phase feedback.

To include the delays in the fast power amplifier feedback, we simply substitute k_0 in (47) by a delay factor.

The loop gain of the fast power amplifier feedback is limited by the delay [8]. Let the stability margin be $\pi/4$, i.e., at the unity loop gain the bandwidth is,

$$\Delta\omega = \frac{\pi}{4\tau} \tag{48}$$

If $2Q\,\Delta\omega > \omega_R$, then the cavity impedance in (11) can be simplified as,

$$Z \approx \frac{R}{j2Q\,\Delta\omega/\omega_R} \tag{49}$$

Therefore, the unity loop gain $|kZ| = 1$ implies,

$$k \leq \frac{\pi Q}{2R\,\omega_R\,\tau} \tag{50}$$

Recalling that $Z_1(s)$ in (36) only represents the dynamic aspect of the cavity response, therefore the static gain of $Z_1(s)$ is 1. On the other hand, the impedance of the cavity at the resonant frequency, and hence the gain, is R. Thus, we find that the fast feedback gain in Fig.10 is,

$$k_0 = kR \leq \frac{\pi Q}{2\omega_R\,\tau} \tag{51}$$

Taking the parameters of the upgraded AGS RF system at injection, if there is a 0.5 μs delay, then the maximum feedback gain k_0 is only 2.2. This is certainly not large enough. If

a gain of better than 10 is required, the total delay in the fast power amplifier feedback should not exceed 113 ns.

Two different kinds of delay exist in the fast power amplifier feedbacks. The first one can be represented by the power amplifier grid resonator, whose model is also a lumped RLC circuit, similar to the one of the cavity. The time constant of this resonator can be reduced by local feedbacks. Using the AGS cavity parameters, closed loop cavity impedances are shown in Fig.12a, where the loop gain at the cavity resonance frequency is the same and the delays are different. In this example, the grid resonator is tuned at the resonance frequency of the cavity, and therefore the two sidebands around the cavity resonance frequency are symmetrical. In Fig.12b, the real part of the impedances in this example are shown. The second kind of delay is the transmission line delay. The closed loop cavity impedances with different delays are shown in Fig.13. In the testing of the AGS upgrade RF fast feedbacks, it is shown [9] that the delay of the grid resonator with local feedbacks is about 80 ns, and the delay of the transmission line is about 30 ns.

In general, if the ratio of the detuned frequency $\Delta\omega$ and the revolution frequency ω_0,

$$\frac{\Delta\omega}{\omega_0} = \frac{I_B R h}{2QV} \cos\phi_S \tag{52}$$

is in the order of unity or larger, then the coupled bunch mode oscillation may be excited, because the cavity impedance may be large at the revolution frequency sidebands. Note here that the equation (52) can be derived from (10) and (15). If a fast feedback is applied, the closed loop cavity impedance in the sidebands shown in Fig.12 and Fig.13 must be considered for the coupled bunch stability.

The feedforward compensation, as commonly introduced for beam loading control, shares basically the same function as the fast power amplifier feedback. The difference is that the correcting signal of the feedforward compensation is picked up from the beam current, whereas for fast feedback it is picked up from the cavity voltage. The drawback of the feedforward technique is that it is difficult to operate over a wide dynamic range.

VIII. Beam Loading with Tuning and AVC Loops

In addition to the fast power amplifier feedback plus the phase and the radial feedbacks, the tuning and AVC feedbacks must also be considered. In general, these two loops have longer time constants, and therefore if only the early short period of beam loading is concerned, they may be totally disregarded. The tuning and AVC loops must however be considered for longer term effect, because the system condition will be largely changed by these two loops.

Immediately after the beam enters the empty cavity, the total cavity voltage starts to move away from the generator induced voltage V_G according to the dynamics represented by $Z_1(s)$ in (36), as shown in Fig.5b. The phase and radial loops observe the increase of the beam phase deviation and start to rotate the RF frequency through the VCO to move the phase of the generator current I_G and the voltage V_G ahead, trying to pull the total cavity voltage V back. Meanwhile, the fast power amplifier feedback observes both phase and amplitude variations in the cavity voltage, and responds by both phase and amplitude corrections in the generator current I_G. The fast power amplifier feedback can usually respond faster than the phase and radial loops. The total effect is shown in Fig.14.

The tuning loop observes the difference between the phases of the generator current I_G and the cavity voltage V. Without fast plus the phase and the radial feedbacks, the phase difference is roughly, disregarding the dynamic aspect, equal to that between I_{G0} and I_T, i.e., ϕ_Z, as shown in Fig.14. With fast plus phase and radial feedbacks, the phase difference is the phase between I_G and V, i.e., ϕ_L. If $\phi_S = 0$, then we have $\phi_L = \phi_Z$. At the injection ϕ_S is small, therefore we always have $\phi_L \approx \phi_Z$. Thus, the fast feedback affects little to the tuning loop.

If we consider that the motion of the phase of the cavity voltage will be delayed, see $Z_1(s)$ in (36), the fast plus phase and radial feedbacks can enhance the difference between the phases of the generator current and the cavity voltage, and therefore enhance the tuning loop reaction [10].

The response of the AVC loop will not be consistent with that of the tuning loop, and it is also less critical than the tuning loop. From the stability point of view, after the cavity is detuned, the situation becomes more complicated. The influence of the beam phase deviation $\Delta\phi_B$ to the phase and the amplitude of the cavity voltage must also be considered. The cross modulation between the phase and the amplitude becomes significant enough and therefore cannot be neglected. The complete stability analysis including all these effects is treated by Pedersen [3].

IX. Conclusion

In this paper, some fundamentals of the beam loading effects have been discussed.

Several issues in the static beam loading such as the cavity detuning condition, the stability condition, and the generator power dissipation are studied. For the transient aspect, we use the beam phase deviation as criterion to present a cavity model and to study the beam loading effect. The old and new AGS RF system parameters are shown as an example to demonstrate how to use the results of the static and transient beam loading study to choose cavity and generator.

Several techniques such as the phase and radial feedbacks, the fast power amplifier feedback and the feedforward compensation have been investigated by using dynamic models. The phase and radial feedbacks have been shown to be not effective enough to correct the beam loading induced beam phase deviation. Increasing the loop gain of these loops will cause unnecessary beam emittance blow up. The fast power amplifier feedback has been shown to be effective in correcting the beam phase deviation. The limitation of the fast feedback due to the time delay is also shown. Finally, the beam loading effect including phase and radial feedbacks, the fast power amplifier feedback, and the tuning and AVC feedbacks is discussed.

X. Acknowledgement

We would like to thank M. Meth, F. Pedersen, W. Pirkl, E. C. Raka, A. Ratti, and R. T. Sanders for helpful discussions.

References

[1] W. T. Weng, *'Fundamentals - Longitudinal Motion,'* AIP Conference Proceedings, 184, pp.243-287, 1989.

[2] K. W. Robinson, *'Stability of Beam in Radiofrequency System,'* CEAL - 1040, 1964.

[3] F. Pedersen, *'Beam Loading Effects in the CERN PS Booster,'* IEEE Trans. On Nuclear Science, Vol.NS-22, pp.1906-1909, 1975.

[4] S. Y. Zhang and W. T. Weng, *'Analysis of Acceleration Control Loops of a Synchrotron,'* Nuclear Instruments & Methods in Physics Research, accepted for publication, May, 1992.

[5] J. G. Truxal, *'Automatic Feedback Control System Synthesis,'* McGraw Hill, New York, 1955.

[6] E. C. Raka, R. Sanders and J. M. Brennan, private communication.

[7] M. Meth and A. Zaltsman, *'Upgrade of AGS RF Cavities for Increased Beam Loading,'* Booster Tech. Note, No.171, BNL, 1990.

[8] D. Boussard, *'Design of a Ring RF System,'* CERN 91-04, 1991.

[9] W. Pirkl and A. Zaltsman, private communication.

[10] J. S. Griffin, *'Compensation for Beam Loading in the 400 GeV Fermilab Main Accelerator,'* IEEE Trans. on Nuclear Science, Vol.NS-22, pp.1910-1913, 1975.

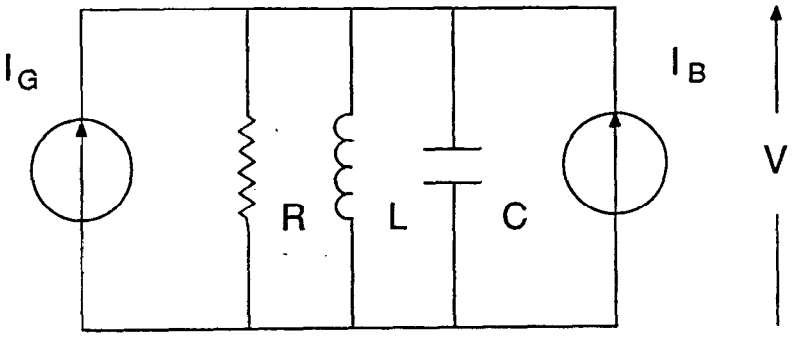

Fig.1. RF Cavity Model.

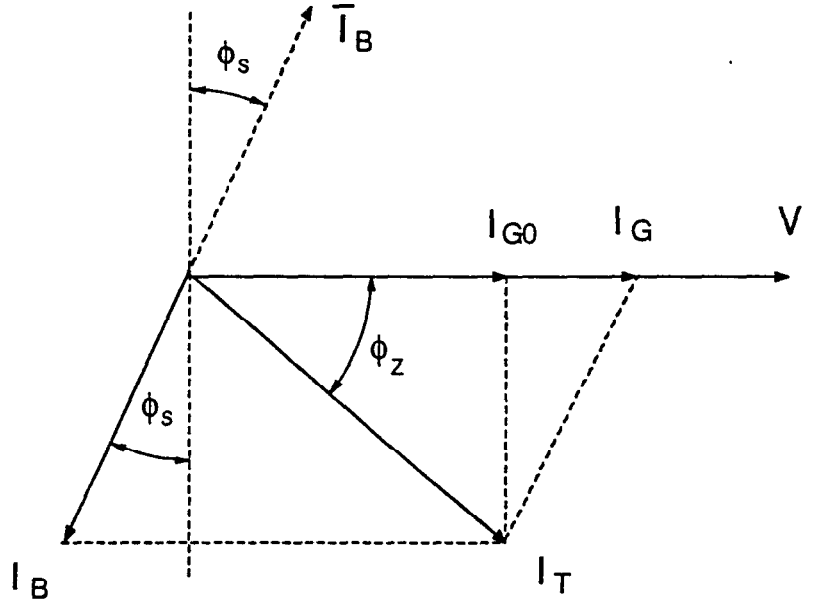

Fig.2. Beam Loading with Cavity Detuning.

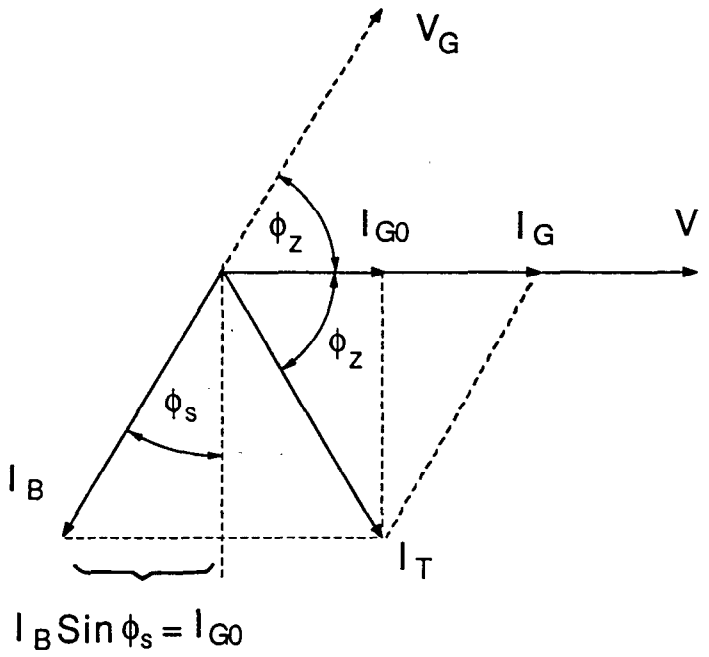

Fig.3. Beam Loading at Stability Limit, the Second Robinson Criterion.

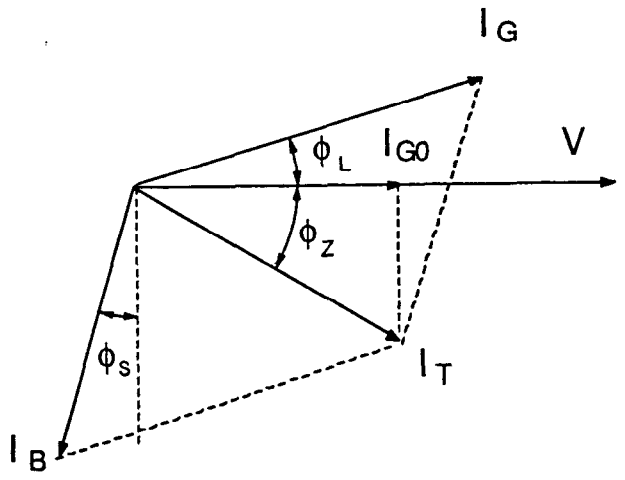

Fig.4. Beam Loading with Partial Cavity Detuning.

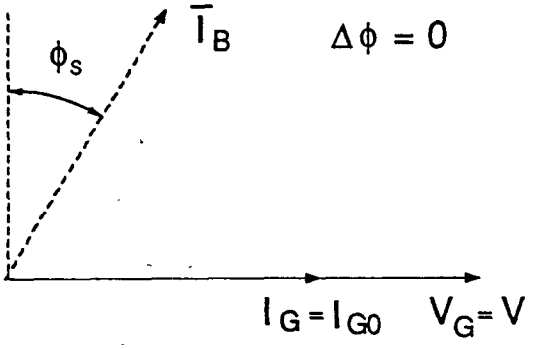

Fig.5a. Beam Phase Deviation without Beam Loading.

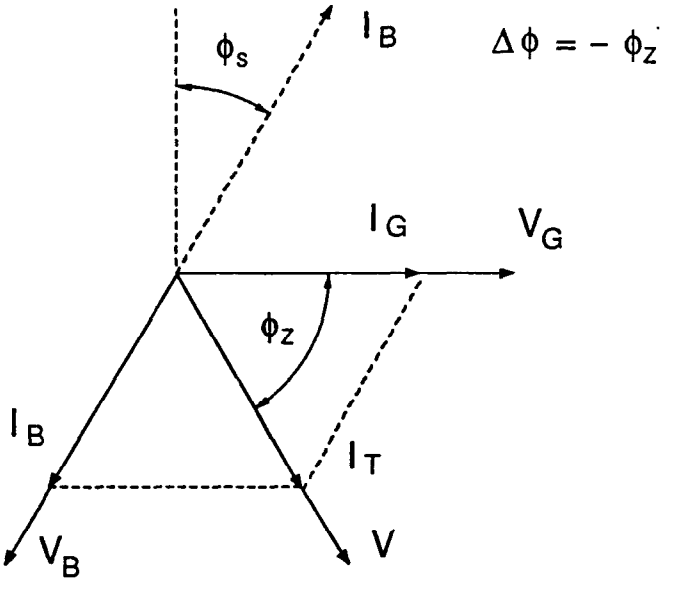

Fig.5b. Beam Phase Deviation with Beam Loading.

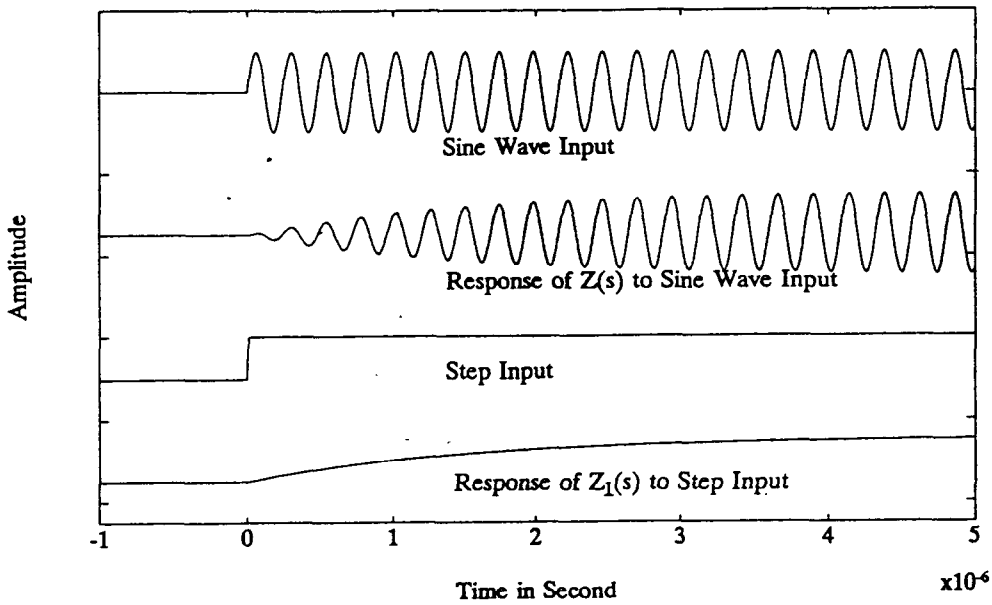

Fig.6. Comparison of the Responses of the Two Cavity Models.

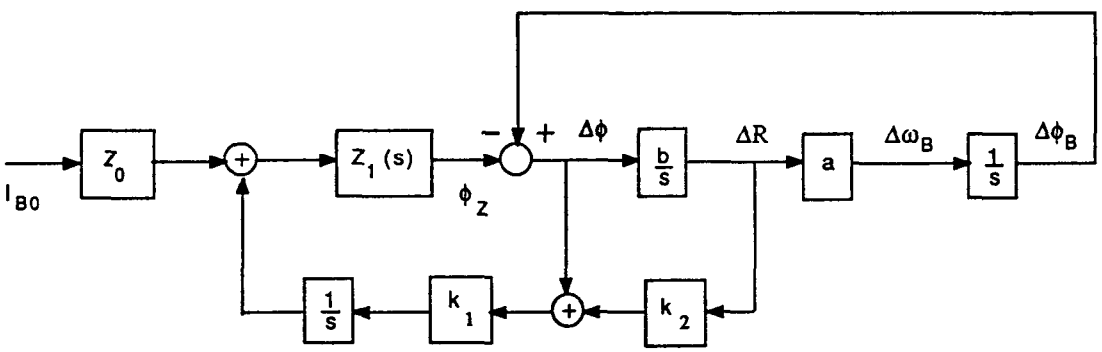

Fig.7. Beam Loading Model with Beam Control.

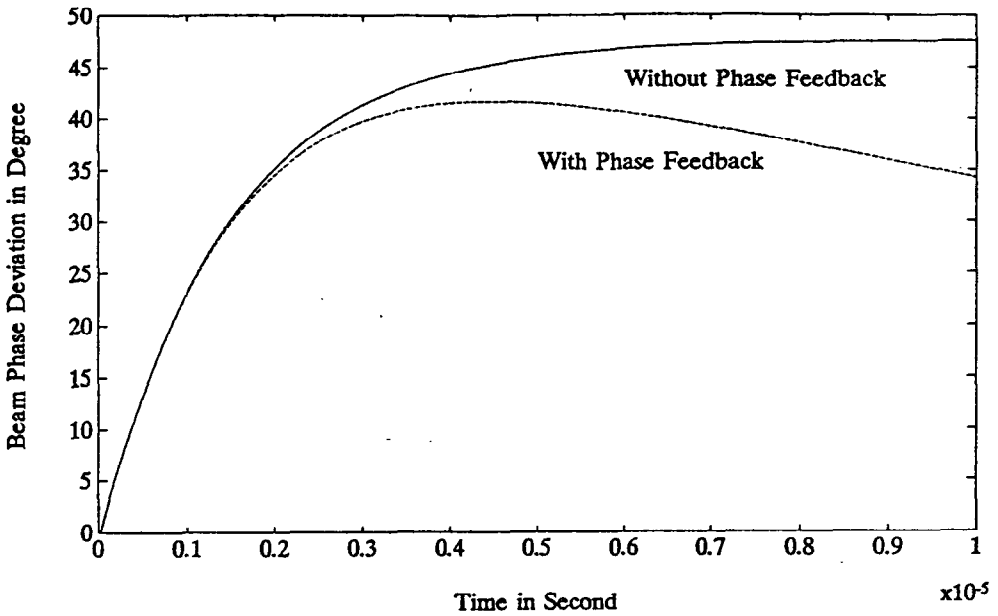

Fig.8. Beam Phase Deviations, with and without Phase and Radial Feedbacks.

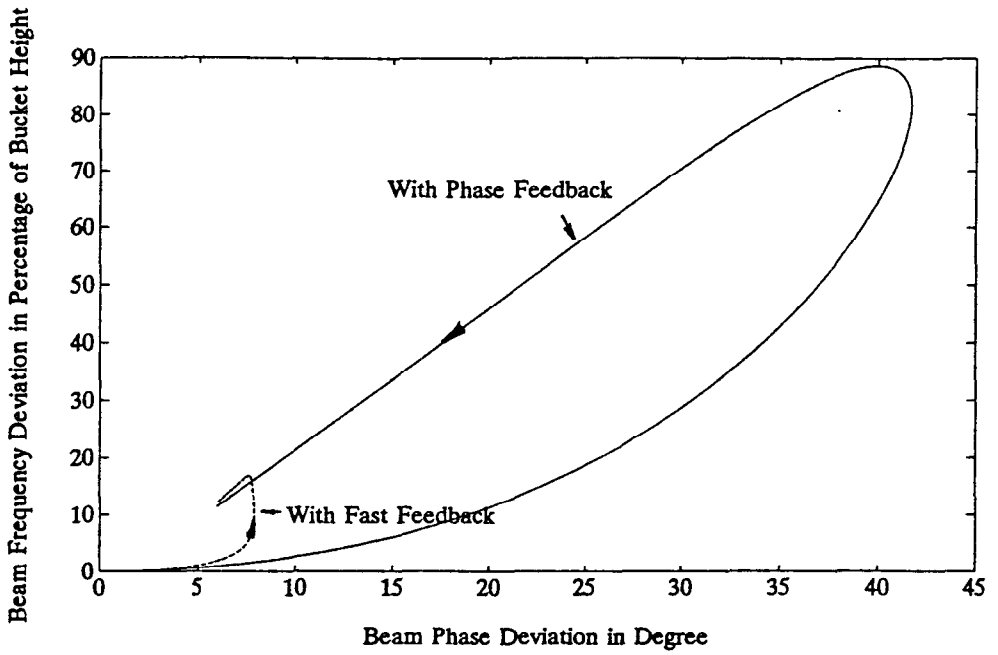

Fig.9. Bunch Motion in the Bucket, with Phase Feedback and Fast Feedback.

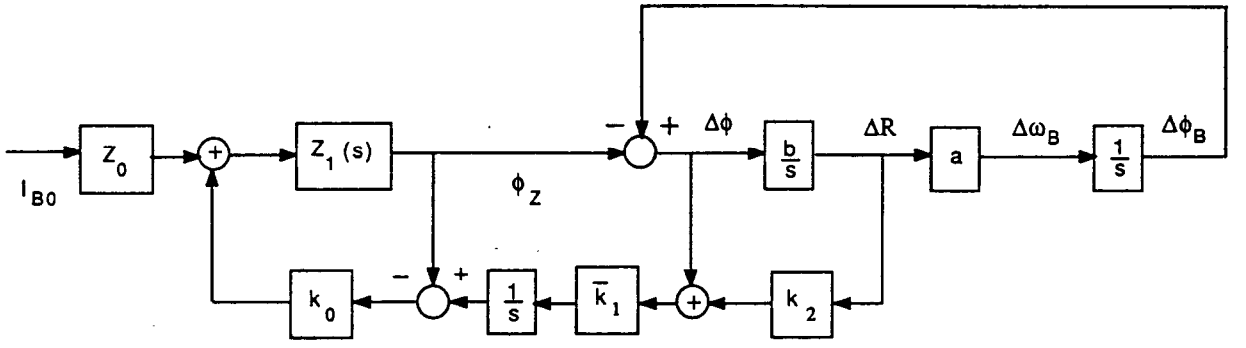

Fig.10. Beam Loading Model with Beam Control and Fast Power Amplifier Feedback.

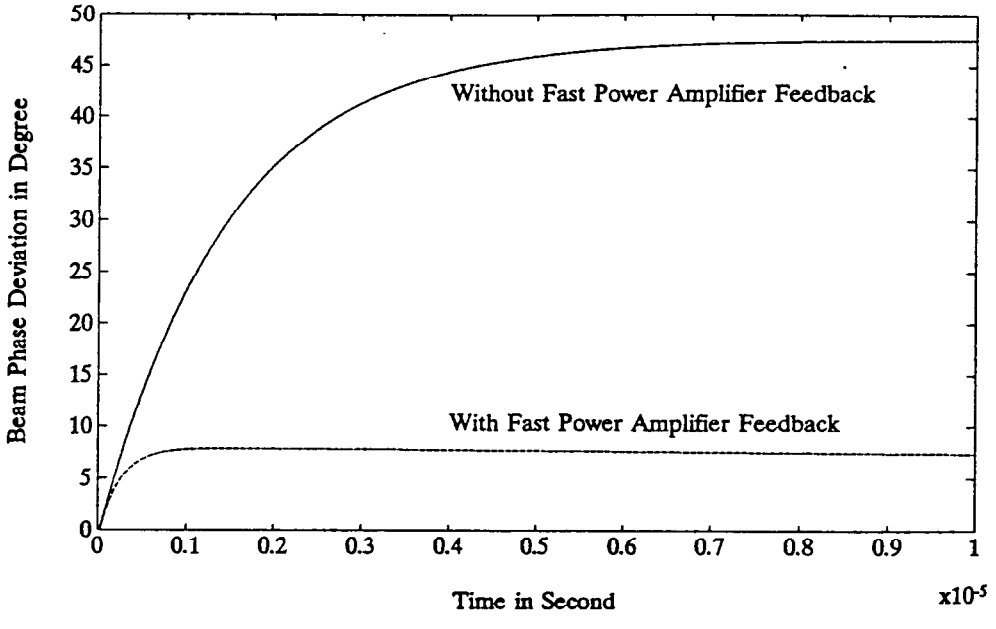

Fig.11. Beam Phase Deviations with and without Fast Power Amplifier Feedback.

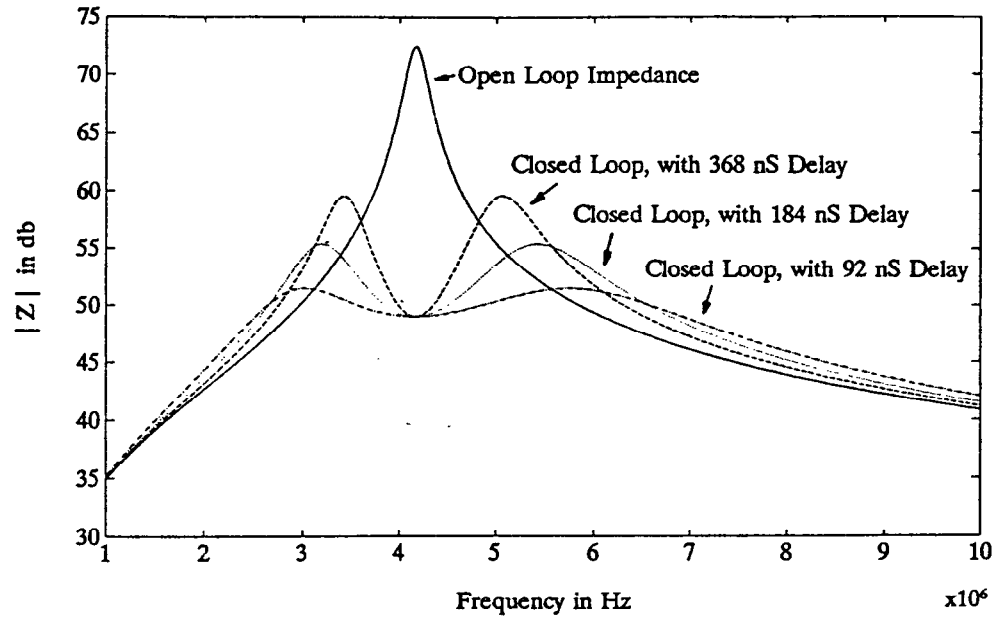

Fig.12a. Cavity Impedance, with Resonator Delays.

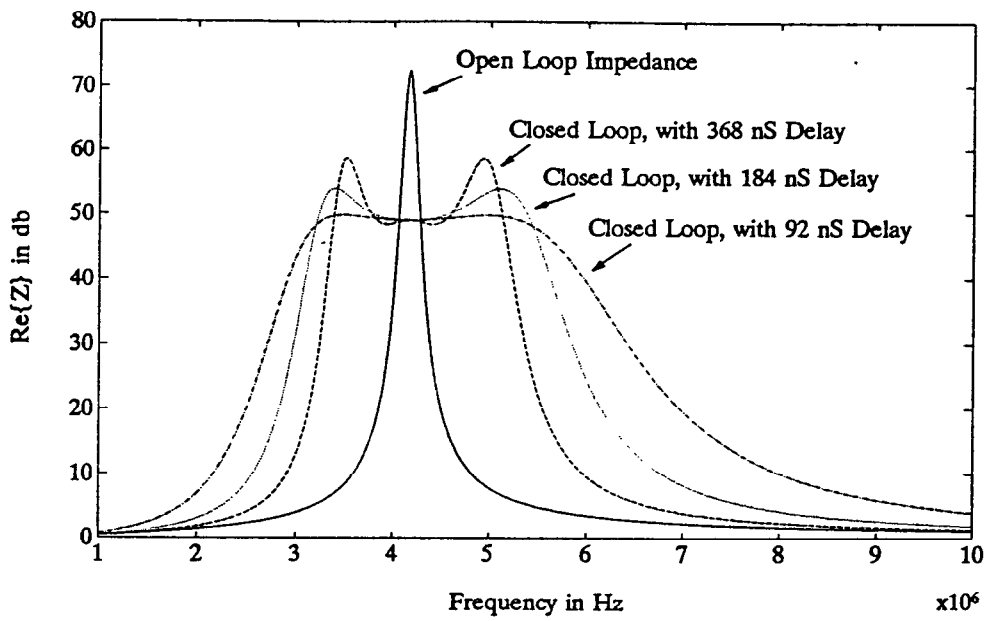

Fig.12b. Real Part of Cavity Impedance, with Resonator Delays.

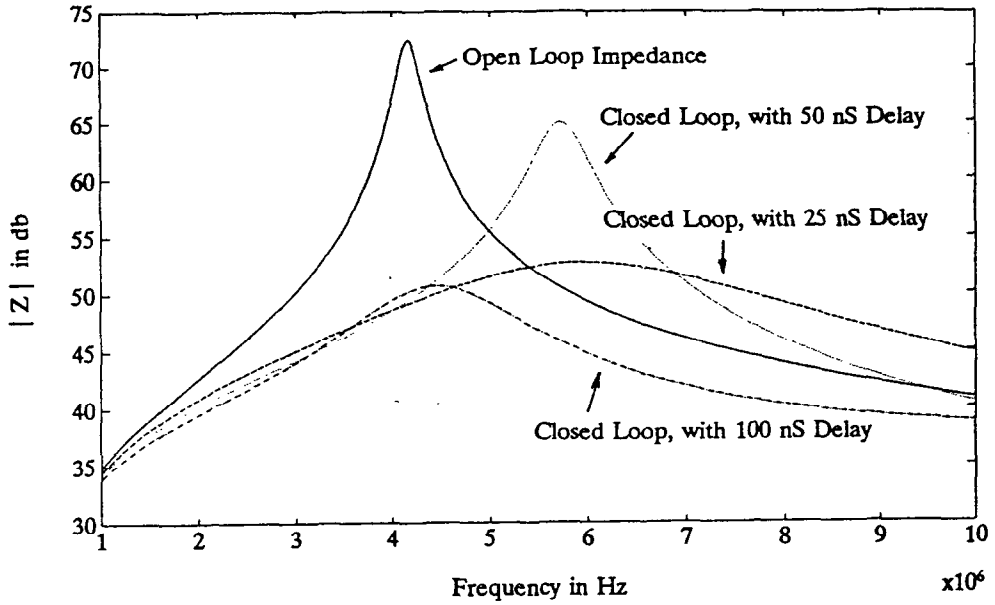

Fig.13. Cavity Impedance, with Transmission Line Delays.

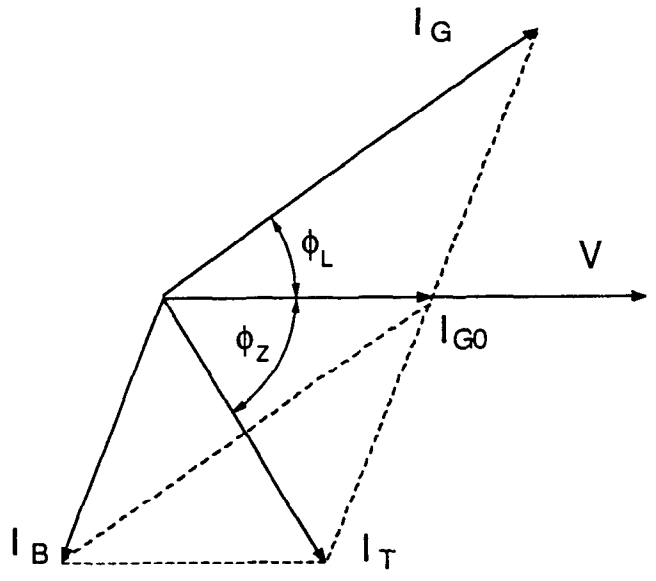

Fig.14. Effect of Fast Power Amplifier Feedback.